Complex Stiffness Gradient Substrates for Studying Mechanotactic Cell Migration

Cheng-Hwa R. Kuo, Jian Xian, James D. Brenton, Kristian Franze, and Easan Sivaniah**

Directed cell migration in response to chemical signals ("chemotaxis") has been extensively studied.[1] In contrast, mechanotaxis (i.e., cellular migration towards mechanical cues) is poorly understood, partly due to a lack of facile methods for generating appropriate cellular environments. Biological tissues are mechanically inhomogeneous;[2,3] particularly during growth and migration, cells are exposed to different mechanical stimuli. The importance of mechanical signaling for cell functioning is becoming increasingly clear. For example, mechanical cues have been shown to direct stem-cell fate,[4] contribute to cancer development,[5] and to influence the growth of nerve-tissue cells.[6] While the number of studies on cellular mechanosensitivity has exploded in recent years, the response of cells to changes in substrate rigidity – despite its potential importance for cell growth and migration – remains sparsely studied.[6] This lack of data may at least partly be attributed to the technical challenges that come with the production of substrates incorporating changes in stiffness while maintaining constant topological and chemical properties.

Currently, most cell-culture substrates used for testing the response of cells to their mechanical environment are made of hydrogels such as polyacrylamide (PAA), polyethylene glycol (PEG), or polydimethylsiloxane (PDMS). Approaches to cell-culture substrates with changes in mechanical properties usually aim at altering the degree of cross-linking in the gel,[7–13] which alters its stiffness. Gradients in cross-linker density are either generated by flowing two sols with different amounts of cross-linking agent into one another or by differentially exposing a photo-crosslinkable gel to UV radiation using a photomask. However, in both instances the gel's mesh size and crosslink-induced surface chemistry will also vary.[14] These substrates are, furthermore, often limited by the minimum possible shear modulus, which is usually in the kilopascal range; the steepness of the gradient, which is usually rather shallow; or the simplicity of the stiffness gradients, which are often linear.

Herein we present a new approach to mechanically complex cell-culture substrates, which overcomes these limitations. This approach is based on the fact that stiff materials can be sensed through soft ones, similar to the fairy-tale princess feeling a pea underneath a pile of mattresses.[12] The amount to which an underlying stiff substrate is felt through a second layer of material depends on the thickness of the superficial compliant layer and the magnitude of its deformation.[15–18] Most tissue cells constantly exert forces on their substrate; the resulting substrate deformation depends on its mechanical properties and the force amplitude. If cells are growing on a compliant gel, which is tightly coupled to an underlying, infinitely stiff material, the gel's apparent stiffness is enhanced as its thickness becomes comparable to the characteristic length scale over which the deformation zone extends.

We employed this phenomenon and built cell-culture substrates with lateral apparent stiffness gradients by varying the height of the superficial compliant material. These variations were achieved by pouring a polymerizing PAA solution onto a glass slide with a topographically patterned surface. After polymerization, the resulting composite materials had a smooth surface; however, the height of the upper, compliant hydrogel layer changed according to the structure of the underlying glass substrate (**Figure 1**).

In this study, we used three different topographically defined glass substrates, which included a step of 100 μm height ("step substrates"); an array of polystyrene spheres of 80 μm diameter ("bead substrates"); and a series of 200 μm wide grooves ("groove substrates") (Figure 1a). Subsequently, we coated these modified substrates with PAA gels of controlled thickness H and known bulk shear modulus G'_{PAA}[19] (Figure 1, Supporting Information, Figure S1). PAA was chosen because of its favorable properties as substrate for cell culture: it provides a diverse range of mechanical compliances covering the elasticity range of most tissue types (0.1–100 kPa), while remaining isotropic and biologically inert. In this study, we used PAA hydrogels with G'_{PAA}= 3.3 k Pa, 10 kPa, and 30 kPa, resembling the stiffness of muscle tissue (≈3–6 kPa),[20] osteoids (>10 kPa),[16] and arteries (≈24–45 kPa)[21] (assuming a Poisson's ratio $\nu = 0.5$): tissues which are in close contact with fibroblasts in vivo.

Thus, the surface of the resulting cell-culture substrates was made of the same material with the same cross-linker density and mesh size; however, the distance between of the gel surface and the underlying glass surface varied across the substrate. This local change in height resulted in a one-dimensional stiffness gradient in case of the step and groove substrates. Moreover, bead substrates incorporated a periodic, two-dimensional, azimuthally symmetric stiffness gradient. To demonstrate this,

C.-H. R. Kuo, Dr. E. Sivaniah
Biological and Soft Systems
Cavendish Laboratory
University of Cambridge, CB3 0HE, UK
E-mail: es10009@cam.ac.uk
Dr. J. Xian, Dr. J. D. Brenton
Cancer Research UK Cambridge Research Institute
Li Ka Shing Centre
Robinson Way, Cambridge CB2 0RE
Dr. K. Franze
Department of Physiology
Development and Neuroscience
University of Cambridge, CB2 3DY, UK
E-mail: kf284@cam.ac.uk

DOI: 10.1002/adma.201202520

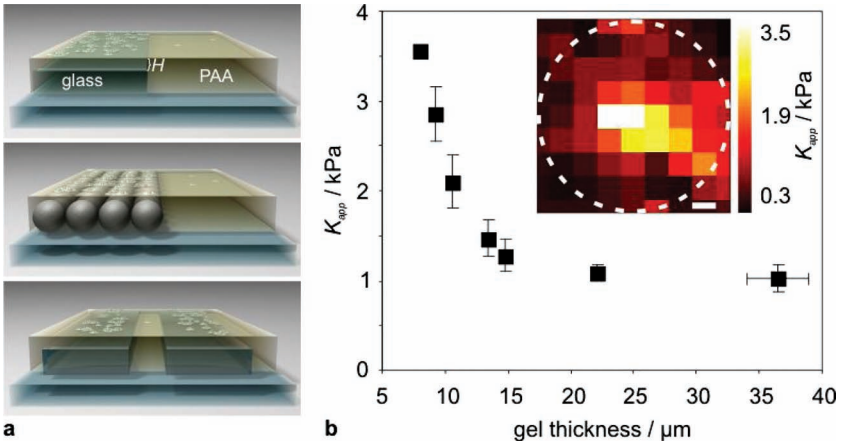

Figure 1. Design of complex mechanical substrates. a) Schematic of different substrates designed for this study. Polyacrylamide (PAA) hydrogel of controlled compliance is polymerized on a topographically patterned stiff support. The resulting variation in gel height H generates apparent stiffness gradients at the substrate surface. The substrates used in this study included 'step substrates', 'bead substrates', and 'groove substrates'. b) Apparent stiffness K_{app} of a "bead substrate", determined by AFM indentation experiments, as a function of gel thickness. The Hertz model was used to fit the raw data at an indentation depth of 1 µm. Inset: apparent stiffness distribution of the substrate over a bead; the bead is indicated by the white broken line. Scale bar: 10 µm.

atomic force microscopy (AFM) was used to measure stiffness maps of the gel surface.[2,3] The Hertz model was used to extract an apparent elastic constant $K_{app} = E/(1 - \nu^2)$ from the raw data, where E and ν are Young's modulus and Poisson's ratio, respectively.[22] Similar to cells, the Hertz model overestimates the true stiffness of a compliant material that is coupled to an underlying stiffer material if the thickness of the compliant material is not much larger than the indentation depth of the probe.[23] Accordingly, K_{app} significantly increased with decreasing gel thicknesses below ≈15 µm, (Figure 1b and Supporting Information, Figure S2 for different indentation depths).

In order to evaluate the suitability of this novel template for mechanotaxis studies, we cultured fibroblasts on the substrates. Fibroblasts are cells found in connective tissue, which is mechanically inhomogeneous. Previously, these cells have been shown to migrate along stiffness gradients.[7] Fibroblasts were first cultured on 'step substrates' for up to 24 h. When the gel thickness H_{step} was larger than ≈15 µm, the cells remained homogeneously distributed across the whole area as quantified by the area-normalized fraction of cells in the shallow region $\varphi_{c,s} = (N_s/A_s)/(N_s/A_s + N_d/A_d) \approx 50\%$, where N refers to cell number, A to the area over which the cell count was performed and d and s denote the deep and shallow zones. However, for substrate areas with $H_{step} < 15$ µm, cells relocated towards the shallower (stiffer) region over a matter of hours of culture (**Figure 2**a). This critical value for H_{step} was similar to the gel thicknesses below which K_{app} increased sharply. We found an inverse relationship between H_{step} and $\varphi_{c,s}$; on the thinnest PAA gels (≈3 µm), between ≈75% and 90% of the cells were located at the apparently stiff region. Surprisingly, $\varphi_{c,s}$ depended only on H_{step} and not on the bulk modulus of the PAA gel (Figure 2b).

One advantage of this method is the ability to create more complex stiffness variations in the cell-culture surface. 'Bead substrates', for example, provide a simple way of engineering substrates incorporating alternating patterns of apparent stiffness. Fibroblasts cultured on these substrates behaved similarly as on step substrates. For $H_{bead} < 15$ µm, cell distributions were again inversely correlated with gel height, with ≈80% of the cells being located on top of the beads at a substrate thickness of ≈3 µm (Figure 2c,d).

To constrain the space available on the apparently softer gel, we then cultured cells on groove substrates (Figure 1a). These substrates were used to test the effect of pharmacological interference with the cells' intrinsic motility machinery on their mechanotactic behavior. Similarly, we investigated how genetic modification of the cells' interaction with their extracellular environment impacts mechanotaxis.

Untreated fibroblasts on groove substrates with $H_{groove} < 15$ µm showed preferential coverage over the non-grooved area (**Figure 3**a,d). Furthermore, their average spreading area $\bar{A}_c$ increased significantly (Figure 3e), which is typical for fibroblasts grown on stiff substrates.[24] On thicker gels, coverage and spreading area were indiscriminate (Figures 3b,e).

The cytoskeleton is crucial for cell motility.[25] To investigate the contribution of its constituents to mechanotactic cell migration, we applied: 1) cytochalasin D (Figure 3c), which inhibits actin polymerization; 2) nocodazole, which induces disassembly of microtubules; or 3) blebbistatin, which blocks the activity of the myosin II motors. All of the independently treated cells were insensitive to the presence of an apparent stiffness gradient, yielding indiscriminate cell coverage over the entire groove substrate area (Figure 3d) and no increase in spreading area (Figure 3e). This insensitivity indicated that all three cytoskeletal components (actin filaments, myosin II motors and microtubules) are required for mechanotactic cell migration.

Transforming growth factor beta induced (TGFBI) is a secreted extracellular-matrix protein that mediates cell adhesion through its interaction with integrins and microtubule stability.[26] It is involved in cell migration, and in cancer cells it may promote invasion and metastasis.[27] To test the importance of cell adhesion for mechanotactic cell migration, we cultured human colorectal DLD1 cells that had been engineered to be TGFBI$^{-/-}$ by homologous recombination on groove substrates. While wild-type DLD1 cells relocated towards the shallow regions of the gel, TGFBI$^{-/-}$ cells homogeneously covered the whole substrate area (Supporting Information, Figure S3), indicating that cell adhesion is crucial for mechanotaxis.

In this study, we developed three simple approaches to fabricate rigidity-patterned cell-culture substrates with homogeneous chemical composition. The slope of the apparent stiffness gradient was altered by the geometry of the underlying stiff substrate: K_{app} will be sharper over an abrupt step if compared to the smoother change in gel height over beads or polymer melts (Supporting Information, Figure S4). These substrates provide promising tools to look into mechanically guided cell

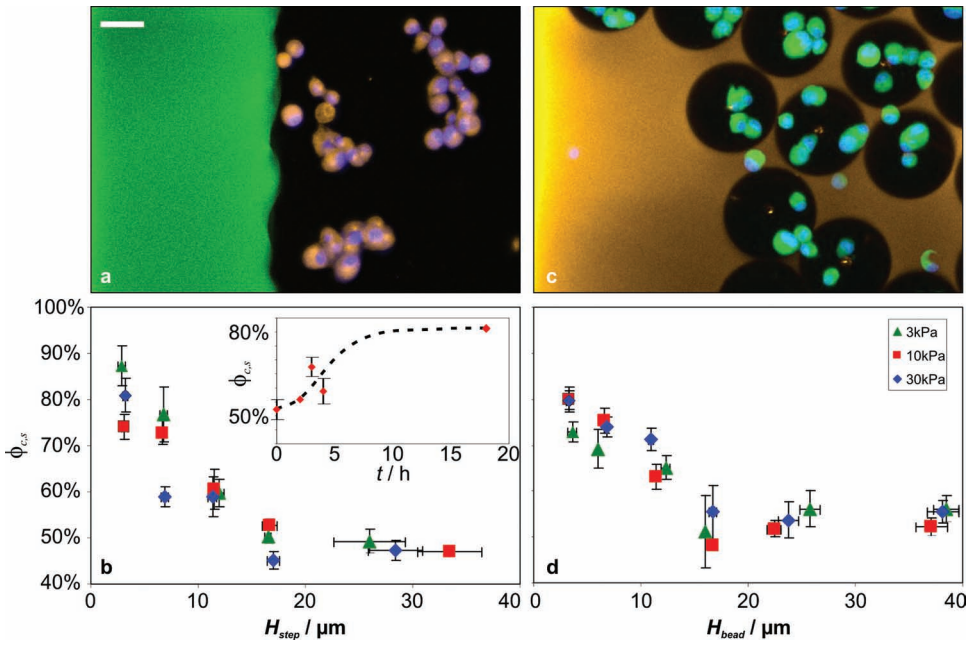

Figure 2. Cell response to complex mechanical substrates. a) Confocal laser scanning microscopy (CLSM) images of fibroblasts growing on a step substrate with $H_{step} = 3$ µm and $G'_{PAA} = 10$ kPa. Cells were labelled with CellTracker Orange (orange), nuclei with Syto 59 (blue). To visualize steps, PAA gels were stained with fluorescein dimethylacrylate (green). The cells are maximum intensity z-projections, the substrates correspond to one optical plane. Fibroblasts relocated towards the apparently stiffer region of the substrate. b) Plot of the area-normalized fraction of cells in the shallow region of the step substrate, $\varphi_{c,s}$, as a function of gel thickness and bulk shear modulus G'_{PAA} (average ± SEM). For gels with $H_{step} < 15$ µm, cells preferentially relocated towards the apparently stiffer shallow region ($N = 45$, 45, and 59 for $G'_{PAA} = 3$, 10, and 30 kPa, respectively; $P < 1 \times 10^{-5}$ for all shear moduli, ANOVA), with more cells relocating with decreasing hydrogel thickness. Within the investigated range this critical thickness was largely independent of the bulk shear modulus G'_{PAA} of the hydrogel ($P > 0.05$ for $H_{step} \neq 7$ µm, ANOVA). The inset shows the temporal development of cell coverage for a step gel with $H_{step} = 10$ µm; the broken line serves as guide to the eye. c) CLSM z-projection of fibroblasts grown on a bead substrate with $H_{bead} = 8$ µm and $G'_{PAA} = 10$ kPa. Cells migrated to the area over the beads where K_{app} is highest. d) Plot of $\varphi_{c,s}$ for bead substrates. For $H_{bead} < 15$ µm, cells accumulated in the apparently stiffer regions ($N = 59$, 89, and 136 for $G'_{PAA} = 3$, 10, and 30 kPa, respectively; $P < 0.01$ for all shear moduli, ANOVA); $\varphi_{c,s}$ increased with further decreasing hydrogel thickness. Again, this critical thickness was independent of the bulk shear modulus of the hydrogel ($P > 0.05$ for all H_{bead}, ANOVA). Scale bar: 50 µm.

migration. In vivo, many cells are constantly exposed to a variety of mechanical cues: tissues are mechanically inhomogeneous at the cellular scale, and local tissue stiffness may change during developmental and pathological events.[6] Many tissue cells respond to their mechanical environment; cellular mechanotaxis may, for example, be involved in wound closure[28] and glial-scar formation after nerve-tissue injuries.[6]

Fibroblasts, which are known to migrate towards increased substrate stiffness,[7,29] recognized and migrated towards the increasing apparent stiffness of their polyacrylamide substrate, whose bulk shear modulus G'_{PAA} was homogeneous but whose depth varied across the surface. We found the critical depth H below which the cells responded to the underlying stiff scaffold to be ≈15 µm, with more cells relocating with decreasing hydrogel thickness. Surprisingly, within the investigated range this critical thickness was largely independent of G'_{PAA}.

The critical depth found in our experiments is in good agreement with previous experiments investigating how deeply cells feel. The substrate height at which cells started to show an increase in area was around 10–20 µm,[17] and cells were suggested to feel the underlying stiff substrate when the gel thickness approaches the lateral cell dimension.[30] In contrast, finite-element computations estimated the critical gel thickness to be 1–2 µm.[15,16] Other studies based on cell-induced traction estimate values on the order of tens of micrometers.[31] However, these values depend on the magnitude of forces exerted by the cells and their adhesion strength.[15]

The apparent substrate stiffness K_{app} that is perceived by a cell is a function of stress σ (i.e., the force it applies to the gel per area, and the resultant strain ε) as $K_{app} = \sigma/\varepsilon$. Thus, K_{app} will be larger if cells exert larger forces (compare also Supporting Information, Figure S2). Different cell types exert different strength forces on their substrates,[32,33] so that substrates should be tailored to the cells of interest. Furthermore, cellular traction forces are dynamic and force magnitudes vary over time.[32] Consequently, K_{app} may vary for a cell within an experiment. While these variations in perceived stiffness cannot experimentally be controlled directly, they partly resemble in vivo conditions where cells are in close contact with the extracellular matrix and other cells whose mechanical properties are often dominated by their cytoskeleton. Similar to the topographically defined substrates presented in this work, extracellular matrix and cytoskeletal proteins stiffen with increasing strain[34] (Supporting Information, Figure S2).

The substrates' apparent stiffness reached the gel's bulk modulus within a few tens of micrometers away from the shallow

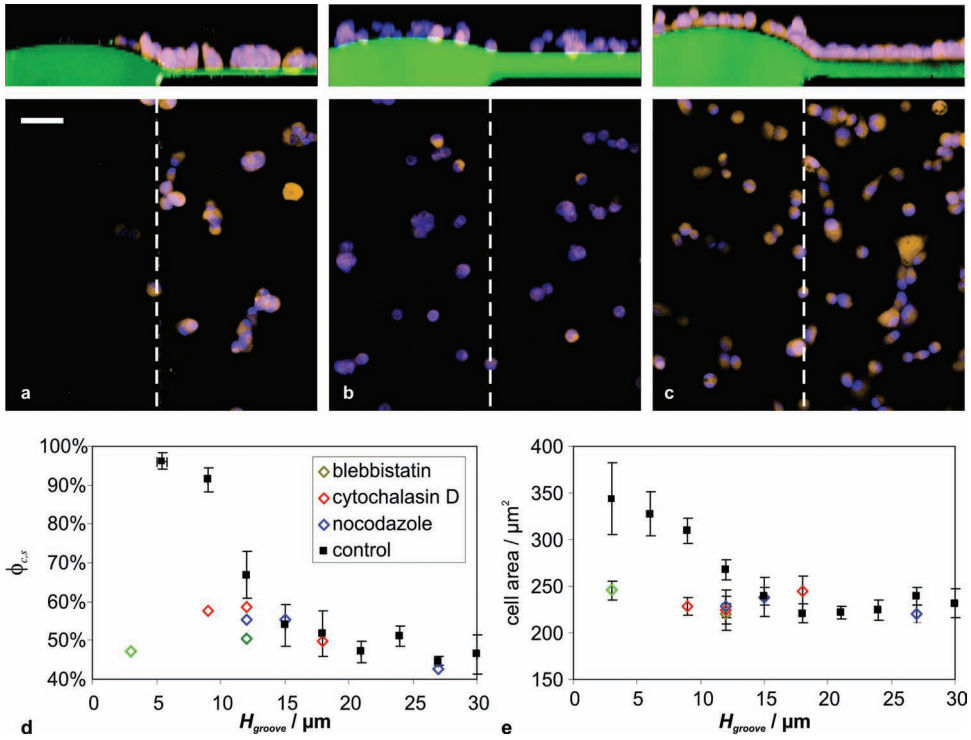

Figure 3. Influence of cytoskeletal components on cellular mechanotaxis. a–c) *y*- (top) and *z*-projections (bottom) of fibroblasts cultured on groove substrates with G'_{PAA} = 10 kPa. The white broken lines indicate the transition between the shallow and the deep regions of the substrate. Scale bar: 50 µm. a) H_{groove} = 6 µm; most cells relocated towards the apparently stiffer region of the substrate. b) H_{groove} = 21 µm; cells no longer responded to the underlying stiff substrate and remained homogeneously distributed. c) Representative image of pharmacologically treated cells. H_{groove} = 12 µm; the fibroblasts were treated with cytochalasin D, which interferes with their actin cytoskeleton. Although H_{groove} was below the critical threshold of ≈15 µm, the cells did not respond to stiffness variations in their substrate. d) Plot of $\varphi_{c,s}$ for groove substrates (G'_{PAA} = 10 kPa). For H_{groove} < 15 µm, untreated cells relocated towards the apparently stiffer region (N = 57, $P < 10^{-15}$, ANOVA); $\varphi_{c,s}$ increased with further decreasing hydrogel thickness. However, when cells were treated with either cytochalasin D, nocodazole, or blebbistatin, cells did not respond to the increasing apparent stiffness of their substrate, indicating that all of the affected components of their cytoskeleton (actin filaments, microtubules, and myosin II motors, respectively) are important for mechanotactic cell migration. e) Similarly, the average spreading area $\bar{A}_c$ of untreated cells increased significantly for H_{groove} < 15 µm (N = 93, P = 0.017, ANOVA), which is typical for fibroblasts grown on and responding to stiff substrates.[24] In contrast, $\bar{A}_c$ of pharmacologically treated cells did not increase (N = 45, P = 0.65, ANOVA), suggesting that all of the investigated cytoskeletal components are involved in cellular mechanosensitivity.

part, making the generated apparent stiffness gradient sharper than what is usually achieved by changing the gels' cross-linker density. However, by varying the topology of the underlying stiff substrates, much shallower gradients can be achieved if desired (Supporting Information, Figure S4). Because the surface of these substrates consists of the same material, cells are not exposed to substrate-mediated differential chemical or topological cues at the cellular scale.[14] A previous study exploiting the principle of layered cell-culture substrates to create stiffness gradients used PDMS as a material that can be patterned using photolithographic techniques.[35] However, the bulk modulus of PDMS is comparatively high, which limits its physiological application to cells found in stiffer tissues such as cartilage or bone.

Due to the nature of hydrogels, thicker portions of the substrates (i.e., larger volume) show a slightly larger degree of swelling than the shallower ones. However, the resulting change in height at the substrate surface has a small slope and occurs over several cell lengths. Furthermore, shallower regions of the gel, which are apparently stiffer, show a concave curvature, which, if at all, should repel cells, which would lead to an underestimation of the number of mechanically guided cells accumulating at shallow gel regions.[36]

In conclusion, we present an elegant application of material physics that allows the projection of an effective stiffness map onto an otherwise homogenous substrate surface using a submerged programmable topography. The production of topographically defined substrates is achievable with lithographic and mold-processing techniques, enabling the fabrication of large amounts and varieties of substrate architectures and hence stiffness patterns. Moreover, these stiffness patterns can be combined with controlled chemical stimuli in a complementary or competing manner. The resulting substrates will offer a complex road-map resembling in vivo conditions more closely than what currently can be achieved. Ultimately, this approach may contribute to the development of a next-generation of biocompatible scaffolds suitable for tissue engineering and biomedical applications.

Experimental Section

Gel and Substrate Preparation: PAA gels of known bulk shear modulus were prepared according to Moshayedi et al.[19] (Supporting Information, Table S1). Briefly, phosphate buffered saline (PBS) (Bioclear), acrylamide

solution (Electran BDH) in PBS, and *N,N′*-methylenebis(acrylamide) (Fisher Scientific) were mixed in appropriate monomer/cross-linker ratios. The gels were fluorescently labeled by addition of fluorescein dimethylacrylate (Aldrich) solution in dimethyl sulfoxide (Sigma). The gel premix was desiccated for 20 min and then gelation initiated by the addition of tetramethyletylenediamine (Argos Organics) accelerator and ammonium persulphate initiator (Sigma). The gel thickness was controlled by altering the volume of pregel mixture added onto topographically patterned substrates before gently sandwiching the gel layer with a further coverslip. To obtain substrates with $H < 15$ μm, ≈10 μL PAA solution were used for the step and bead substrates and ≈30 μL for groove substrates. After gelation, the substrates were soaked in PBS for 2 h followed by the gentle removal of the top coverslips. To functionalize the surface and facilitate cell adhesion, the substrates were then soaked in hydrazine hydrate (Aldrich) for 16 h, followed by washing in 5% acetic acid (1 h) and sterile PBS before treatment with poly(D-lysine) (PDL) (100 μg mL^{-1}, Sigma) in PBS. Finally, substrates were washed in PBS and cell-culture medium and then cells were added.

Step substrates were prepared by gluing two overlapping coverslips together (using UV adhesives; Northland UV-cured Adhesive 81). Bead substrates were prepared by depositing and drying a dilute solution of mondisperse polystyrene spheres (80 μm diameter, 8 wt% in absolute ethanol; Duke Scientific ltd.) on coverslips. Slow air drying enabled the surface tension of the solvent to gently pull individual polystyrene spheres together as it evaporated away, leaving behind a densely packed monolayer array of beads. These spheres were briefly heat treated to ensure adhesion to themselves and the glass surface. Groove substrates were custom-made from microscope glass slides (UQG Optics ltd.) using a diamond saw to create a 200 μm deep and 150 or 200 μm wide grooves that were 2 mm apart, and 2 cm long. To allow the PAA gel to adhere to these structures, substrates were chemically treated as previously described.[19]

Cell Culture: 3T3 fibroblasts (ATCC: CCL-92) and DLD-1 colorectal adenocarcinoma cells were grown in polystyrene flasks between passages 2 and 20 in a humidified 37 °C, 5% CO_2 incubator using modified Dulbecco's Modified Eagle's Medium (DMEM) (Invitrogen) for fibroblasts and RPMI-1640 medium (Invitrogen) for DLD-1 cells. DLD-1 colorectal adenocarcinoma cell-line wild-type and $TGFBI^{-/-}$ cells were produced by homologous recombination. The strategy for generating gene-targeting constructs was described by others.[37] Using polymerase chain reaction (PCR), regions of homology at the TGFBI loci were amplified from genomic DNA extracted from DLD1 cells. NotI sites were embedded within the primers used to amplify homology arms. Targeting constructs were generated by fusion PCR, which links homology arms and selectable marker gene cassettes. The targeting plasmid pAAV-TGFBI (AAV: adeno-associated viral) was assembled by ligation of fusion PCR product into pAAV-MCS (MCS: multiple cloning site), an AAV shuttle vector that carries two inverted terminal repeats (ITR) sequences necessary for viral packaging (Stratagene). The selectable marker gene cassette contained neomycin resistant or hygromycin B resistant gene flanked by lox*P* sites. The cells were fluorescently labeled with CellTracker Orange CMRA (C34551, Invitrogen) and Hoechst 33342 (H3570, Invitrogen) or Syto 59 (red fluorescent, S11341, Invitrogen). Stained cells were resuspended in fresh culture medium, 100 μL of which (5×10^5 cells mL^{-1}) were added onto the PDL-coated substrates. After allowing 10 min for cells to settle onto the gel surface, petri dishes were filled with fresh cell-culture medium and incubated for 24 h before imaging. In a set of experiments, cells were treated with blebbistatin (1×10^{-6} M, Sigma), cytochalasin D (1×10^{-6} M, Sigma), or nocodazole (1×10^{-6} M, Sigma) for 1 h inside an incubator prior to staining and seeding using the same protocol as mentioned above.[25]

Imaging and Analysis: AFM measurements were carried out as previously described.[2,3] Monodisperse polystyrene beads (diameter 5.46 μm ± 0.12 μm, microParticles GmbH, Berlin, Germany) were glued to silicon cantilevers (spring constant ≈0.1 N m^{-1}) (PPP-BSI, Nanosensors, Neuchatel, Switzerland). Cantilevers were mounted on a Nanowizard III AFM (JPK Instruments AG, Berlin, Germany), which was setup on an inverted microscope (AxioObserver A1, Zeiss, UK). Force–distance curves were recorded every 10 μm within arrays of 100 × 100 μm (Figure 1b inset); phase-contrast microscopy was used at the same time to visualize the position on the substrate. Data were analyzed for up to 1 μm indentation depths using a custom algorithm based in Matlab (MathWorks, Natick, USA),[2] which fitted the data with the Hertz model.[22]

Optical imaging was performed using a Zeiss LSM-510 Meta confocal laser scanning microscope with a 25× objective (water immersion, NA = 0.8). *Z*-stacks were acquired at randomly selected areas along the transition zone between shallow and deep regions of the gels. The gel thickness *H* was measured using a 3D reconstruction of the *z*-stacks. Image stacks were further processed and analyzed using ImageJ to determine the pattern coverage area and total cell counts. The statistical significance of the cell coverage was determined using analysis of variance (ANOVA).

Supporting Information

Supporting Information is available from the Wiley Online Library or from the author.

Acknowledgements

The authors would like to thank Jochen Guck and Krystyn Van Vliet for valuable discussions and Jens Grosche (Effigos AG) for providing Figure 1a. This work was supported by funding by the EPSRC, and an MRC Career Development Award (to K.F.).

Received: June 21, 2012
Revised: August 14, 2012
Published online: September 18, 2012

[1] N. Li Jeon, H. Baskaran, S. K. Dertinger, G. M. Whitesides, L. Van de Water, M. Toner, *Nat. Biotechnol.* **2002**, *20*, 826.
[2] A. F. Christ, K. Franze, H. Gautier, P. Moshayedi, J. Fawcett, R. J. Franklin, R. T. Karadottir, J. Guck, *J. Biomech.* **2010**, *43*, 2986.
[3] K. Franze, M. Francke, K. Günter, A. F. Christ, N. Körber, A. Reichenbach, J. Guck, *Soft Matter* **2011**, *7*, 3147.
[4] A. J. Engler, S. Sen, H. L. Sweeney, D. E. Discher, *Cell* **2006**, *126*, 677.
[5] M. J. Paszek, N. Zahir, K. R. Johnson, J. N. Lakins, G. I. Rozenberg, A. Gefen, C. A. Reinhart-King, S. S. Margulies, M. Dembo, D. Boettiger, D. A. Hammer, V. M. Weaver, *Cancer Cell* **2005**, *8*, 241.
[6] K. Franze, J. Guck, *Rep. Prog. Phys.* **2010**, *73*, 094601.
[7] C. M. Lo, H. B. Wang, M. Dembo, Y. L. Wang, *Biophys. J.* **2000**, *79*, 144.
[8] S. Kidoaki, T. Matsuda, *J. Biotechnol.* **2008**, *133*, 225.
[9] B. C. Isenberg, P. A. Dimilla, M. Walker, S. Kim, J. Y. Wong, *Biophys. J.* **2009**, *97*, 1313.
[10] F. J. Byfield, Q. Wen, I. Levental, K. Nordstrom, P. E. Arratia, R. T. Miller, P. A. Janmey, *Biophys. J.* **2009**, *96*, 5095.
[11] S. Sant, M. J. Hancock, J. P. Donnelly, D. Iyer, A. Khademhosseini, *Can. J. Chem. Eng.* **2010**, *88*, 899.
[12] J. R. Tse, A. J. Engler, *Preparation of Hydrogel Substrates with Tunable Mechanical Properties*, *Current Protocols in Cell Biology*, **2010**, *47:10.16.1–10.16.16*; DOI: 10.1002/0471143030.cb1016s47.
[13] S. Nemir, H. N. Hayenga, J. L. West, *Biotechnol. Bioeng.* **2010**, *105*, 636.
[14] B. Trappmann, J. E. Gautrot, J. T. Connelly, D. G. Strange, Y. Li, M. L. Oyen, M. A. Cohen Stuart, H. Boehm, B. Li, V. Vogel, J. P. Spatz, F. M. Watt, W. T. Huck, *Nat. Mater.* **2012**, *11*, 742.
[15] J. M. Maloney, E. B. Walton, C. M. Bruce, K. J. Van Vliet, *Phys. Rev. E* **2008**, *78*, 041923.

[16] S. Sen, A. J. Engler, D. E. Discher, *Cell. Mol. Bioeng.* **2009**, *2*, 39.
[17] A. Buxboim, K. Rajagopal, A. E. X. Brown, D. E. Discher, *J. Phys.: Condens. Matter* **2010**, *22*, 1.
[18] W. T. Chen, *Int. J. Eng. Sci.* **1971**, *9*, 775.
[19] P. Moshayedi, L. D. Costa, A. Christ, S. P. Lacour, J. Fawcett, J. Guck, K. Franze, *J. Phys.: Condens. Matter* **2010**, *22*, 194114.
[20] A. J. Engler, M. A. Griffin, S. Sen, C. G. Bonnemann, H. L. Sweeney, D. E. Discher, *J. Cell. Biol.* **2004**, *166*, 877.
[21] M. Bernal, I. Nenadic, M. W. Urban, J. F. Greenleaf, *J. Acoust. Soc. Am.* **2011**, *129*, 1344.
[22] H. Hertz, *J. Reine Angew. Math.* **1881**, *92*, 156.
[23] K. Franze, *Curr. Opin. Genet. Dev.* **2011**, *21*, 530.
[24] T. Yeung, P. C. Georges, L. A. Flanagan, B. Marg, M. Ortiz, M. Funaki, N. Zahir, W. Ming, V. Weaver, P. A. Janmey, *Cell Motil. Cytoskeleton* **2005**, *60*, 24.
[25] J. da Silva, F. Lautenschlager, C. H. Kuo, J. Guck, E. Sivaniah, *Integr. Biol.* **2011**, *3*, 1202.
[26] A. A. Ahmed, A. D. Mills, A. E. Ibrahim, J. Temple, C. Blenkiron, M. Vias, C. E. Massie, N. G. Iyer, A. McGeoch, R. Crawford, B. Nicke, J. Downward, C. Swanton, S. D. Bell, H. M. Earl, R. A. Laskey, C. Caldas, J. D. Brenton, *Cancer Cell* **2007**, *12*, 514.
[27] C. Ma, Y. Rong, D. R. Radiloff, M. B. Datto, B. Centeno, S. Bao, A. W. Cheng, F. Lin, S. Jiang, T. J. Yeatman, X. F. Wang, *Genes Dev.* **2008**, *22*, 308.
[28] T. E. Angelini, E. Hannezo, X. Trepat, J. J. Fredberg, D. A. Weitz, *Phys. Rev. Lett.* **2010**, *104*, 168104.
[29] D. S. Gray, J. Tien, C. S. Chen, *J. Biomed. Mater. Res.* **2003**, *66*, 605.
[30] Y. C. Lin, D. T. Tambe, C. Y. Park, M. R. Wasserman, X. Trepat, R. Krishnan, G. Lenormand, J. J. Fredberg, J. P. Butler, *Phys. Rev. E* **2010**, *82*, 041918.
[31] R. Merkel, N. Kirchgebner, C. M. Cesa, B. Hoffmann, *Biophys. J.* **2007**, *93*, 3314.
[32] T. Betz, D. Koch, Y. B. Lu, K. Franze, J. A. Kas, *Proc. Natl. Acad. Sci. USA* **2011**, *108*, 13420.
[33] B. Sabass, M. L. Gardel, C. M. Waterman, U. S. Schwarz, *Biophys. J.* **2008**, *94*, 207.
[34] C. Storm, J. J. Pastore, F. C. MacKintosh, T. C. Lubensky, P. A. Janmey, *Nature* **2005**, *435*, 191.
[35] B. Cortese, G. Gigli, M. Riehle, *Adv. Funct. Mater.* **2009**, *19*, 2961.
[36] J. Y. Park, D. H. Lee, E. J. Lee, S. H. Lee, *Lab Chip* **2009**, *9*, 2043.
[37] M. Kohli, C. Rago, C. Lengauer, K. W. Kinzler, B. Vogelstein, *Nucleic Acids Res.* **2004**, *32*, e3.